Modeling an Off-Nominal Launch Vehicle Trajectory for Range Safety Link Analysis

Joseph C. Chen, Charles C. Wang, David Taggart, Ed Ditata
The Aerospace Corporation
El Segundo, California
Phone: (310) 336-8774
Email: chen-tsing.chen@aero.org

Abstract - The dynamic link analysis for the Telemetry and Command subsystems is frequently required to ensure adequate link closure for range safety. This analysis takes into consideration vehicle antenna patterns, locations of ground stations, and dynamics of launch vehicles (pitch-roll-yaw and position) of a nominal launch trajectory. However, for the purpose of range safety, the link analysis of an off-nominal trajectory is even more critical than that for the nominal one because that is when the Command Destruct signal will be most likely sent (if the vehicle is heading to a populated area).

An off-nominal trajectory may be a simple heading change from the planned route, or it may consist of a series of vehicle tumbles. In this paper, a three-step algorithm is developed to model an off-nominal trajectory. Based on the algorithm, a tool is developed to generate off-nominal trajectories, which are in turn used for dynamic link analysis. This tool provides a powerful capability for system analysts to decide the destruct lines and perform engineering trade studies over a wide range of trajectories.

TABLE OF CONTENTS

1. INTRODUCTION

The Telemetry and Command subsystems constitute two of the most important subsystems of the U.S. Air Force Spacelift Range System (SLRS) designed to provide operational support for the space launch vehicles. A command destruct signal (CDS) is sent to the space vehicle if the trajectory of the space vehicle poses any serious safety concerns [1]. Presently the U.S. Air Force is in the process of upgrading and modernizing the equipment at the tracking sites. Therefore, a thorough analysis is required to ensure that the command uplink can be closed with sufficient margin under the worst possible conditions and from any intended ground site(s). The worst possible conditions include trajectories of a vehicle that experiences a loss control, which may include a sudden heading change to a populated area or may consist of a series of tumbles.

Several simulation tools were developed at The Aerospace Corporation for the detailed modeling of the CDS Subsystem. One of the simulation tools developed is the Matlab-based link margin calculation program, which is capable of performing detailed link calculations for the nominal launch trajectory, as well as for an off-nominal trajectory under a multitude of specified parameters [2]. These parameters include the location of the launch site and command destruct sites, dynamics of launch vehicles, the command receiver antenna characteristics, and its mounting onboard the launch vehicles. Other important parameters include the propagation loss through plume derived from various plume models and the gain pattern of ground station transmit antenna.

Another important tool developed is the Matlab-based off-nominal trajectory program, which is capable of generating the off-nominal trajectories based on a three-step algorithm. Step 1 is to prepare the necessary dynamic parameters for the nominal trajectory in Earth-fixed coordinates, such as Earth-centered Earth-fixed (ECEF) coordinates or local-level coordinates, which are rotating with the Earth. These parameters include the position in geodetic coordinates, and the local-level velocity and acceleration vectors. In order to keep track of the vehicle orientation, it is necessary to derive vehicle attitude angles and attitude rates. Step 2 is to apply the desired maneuvers such as changes of attitude rate or acceleration onto the nominal trajectory, and re-compute the dynamic parameters mentioned in Step 1 for the off-nominal trajectory. Step 3 is to transform the dynamic parameters from ECEF coordinates back to Earth-centered inertial (ECI) coordinates, which are commonly used in the space vehicle application.

2. A THREE-STEP ALGORITHM

The nominal space vehicle trajectory is frequently described by dynamics parameters expressed in coordinates relative to the inertial frame. The parameters include the position in

[1] 0-7803-7651-X/03/$17.00 © 2003 IEEE
[2] IEEEAC paper #256, Updated December 10, 2002

ECI coordinates, the acceleration vector sensed by an accelerometer triad, the body rate vector sensed by a gyro triad, and the transformation matrix from the inertial frame to the vehicle body frame at low data rate, such as 1 Hz. Since modeling of the off-nominal trajectory is accomplished by inserting the desired maneuvers onto an existing trajectory, it is often acceptable to take the low-rate data as input. If a more accurate trajectory is demanded by the link analysis, a higher data rate will be required. The three-step algorithm using the available input data can be described in detail as follows.

Step 1: Prepare the dynamic parameters of the nominal trajectory in Earth-fixed coordinates, which are rotating with respect to inertial space. It is convenient to work on parameters in Earth-fixed frames, which are commonly used in the terrestrial application.

First of all, convert the position in ECI coordinates to geodetic latitude, longitude, and altitude with the following equations [3].

$$\begin{bmatrix} x_e \\ y_e \\ z_e \end{bmatrix} = \underbrace{\begin{bmatrix} \cos\Omega t & \sin\Omega t & 0 \\ -\sin\Omega t & \cos\Omega t & 0 \\ 0 & 0 & 1 \end{bmatrix}}_{C_i^e} \begin{bmatrix} x_i \\ y_i \\ z_i \end{bmatrix} \tag{1}$$

and

$$\begin{bmatrix} x_e \\ y_e \\ z_e \end{bmatrix} = \begin{bmatrix} (R+h)\cos\Phi_c \cos\lambda_c \\ (R+h)\cos\Phi_c \sin\lambda_c \\ (R+h)\sin\Phi_c \end{bmatrix} \tag{2}$$

where $\left[x_i, y_i, z_i\right]^T$ = position in ECI frame
$\left[x_e, y_e, z_e\right]^T$ = position in ECEF frame
C_i^e = transformation matrix from ECI frame to ECEF frame
Ω = the Earth rotation rate
Φ_c = geocentric latitude
λ_c = geocentric longitude
R = the Earth radius
h = vehicle altitude

The geodetic location can also be obtained from the following equation [3].

$$\begin{bmatrix} x_e \\ y_e \\ z_e \end{bmatrix} = \begin{bmatrix} (R_\lambda + h)\cos\Phi\cos\lambda \\ (R_\lambda + h)\cos\Phi\sin\lambda \\ \left[\left(1-\varepsilon^2\right)R_\lambda + h\right]\sin\Phi \end{bmatrix} \tag{3}$$

where R_λ = the radius of curvature in the east-west direction
ε^2 = reference ellipsoid eccentricity squares
Φ = geodetic latitude
λ = geodetic longitude

Secondly, compute the vehicle velocity vector and the craft rate vector relative to the Earth in a local-level frame using the acceleration vector sensed by the accelerometer triad.

The generalized navigation equation for a vehicle, which is referenced to the Earth, can be expressed in local-level coordinates (L or l) [3].

$$\left[{dv}/{dt}\right]_l = A - (\rho + 2\Omega)\times v + g \tag{4}$$

where v = velocity of the vehicle with respect to the Earth
A = nongravitational specific force or the acceleration vector sensed or measured by an accelerometer triad
$(\rho + 2\Omega)\times v$ = the gravity contribution due to the Coriolis and centripetal effect of velocity
ρ = the transport rate or craft rate
g = the gravity vector, which combines the mass attraction gravitation term and the centripetal acceleration due to the Earth's rotation

The craft rate, the angular rate of a local-level platform with respect to the rotating Earth, can be expressed in the form

$$\rho = {v}/{(R+h)} \tag{5}$$

The gravity vector, which combines the mass attraction term and the centripetal acceleration, is in the form of

$$g = g_m - \Omega\times\left(\Omega\times R\right) \tag{6}$$

where g_m = the gravity mass attraction term.

Thirdly, derive the vehicle attitude angles from the transformation matrix from the local-level frame to the body frame, and compute the attitude rates from the body rates, relative to the local-level frame and expressed in the body frame.

The attitude angles, pitch, roll, and yaw angles, can be obtained from C_l^b, which will be defined in equation (8).

Thus $$\theta = \tan^{-1}\left[\frac{-C_{13}}{\sqrt{1-C_{13}^2}}\right] \quad (7)$$

$$\phi = \tan^{-1}\left(\frac{C_{23}}{C_{33}}\right),\ \psi = \tan^{-1}\left(\frac{C_{12}}{C_{11}}\right)$$

where $\phi, \theta,$ and ψ denote roll, pitch, and yaw angles, respectively.

The transformation matrix from the local-level frame to the body frame is given in the form of

$$C_l^b = \begin{bmatrix} \cos\theta\cos\psi & \cos\theta\sin\psi & -\sin\psi \\ (\sin\phi\sin\theta\cos\psi \\ -\cos\phi\sin\psi) & (\sin\phi\sin\theta\sin\psi \\ +\cos\phi\cos\psi) & \sin\phi\cos\theta \\ (\cos\phi\sin\theta\cos\psi \\ +\sin\phi\sin\psi) & (\cos\phi\sin\theta\sin\psi \\ -\sin\phi\cos\psi) & \cos\phi\cos\theta \end{bmatrix}$$

(8)

The above transformation matrix can be computed from

$$C_l^b = C_i^b C_i^{e^T} C_e^{l^T} \quad (9)$$

where C_i^b = Transformation matrix from ECI to body frame, the given parameters of nominal trajectory

C_i^e = Transformation matrix from ECI to ECEF frame given in equation (1)

C_e^l = Transformation matrix from ECEF frame to local-level frame in (north, west, up)

The transformation matrix from the ECEF frame to the local- level frame can be obtained by

$$C_e^l = \begin{bmatrix} -\sin\Phi\cos\lambda & -\sin\Phi\sin\lambda & \cos\Phi \\ \sin\lambda & -\cos\lambda & 0 \\ \cos\Phi\cos\lambda & \cos\Phi\sin\lambda & \sin\Phi \end{bmatrix} \quad (10)$$

where Φ = geodetic latitude

λ = geodetic longitude

The attitude rates can be obtained from the following equation:

$$\frac{d}{dt}\begin{bmatrix}\phi \\ \theta \\ \psi\end{bmatrix} = \begin{bmatrix} 1 & \tan\theta\sin\phi & \tan\theta\cos\phi \\ 0 & \cos\phi & -\sin\phi \\ 0 & \dfrac{\sin\phi}{\cos\theta} & \dfrac{\cos\phi}{\cos\theta} \end{bmatrix}\begin{bmatrix}P \\ Q \\ R\end{bmatrix} \quad (11)$$

where $(P,Q,R)^T = \omega_{lb}^b$ = body angular rate relative to the local-level frame expressed in the body frame.

The input platform rates $(P,Q,R)^T$ can be computed from

$$\omega_{lb}^b = \omega_{ib}^b - \omega_{ie}^b - \omega_{el}^b = \omega_{ib}^b - \Omega^b - \rho^b \quad (12)$$

where ω_{ib}^b = body angular rates relative to inertial space expressed in body frame, the given body rate vector sensed by a gyro triad

$\omega_{ie}^b = \Omega^b$ = Earth rotation rate relative to inertial space expressed in body frame

$\omega_{el}^b = \rho^b$ = craft rate relative to the Earth expressed in body frame

Figure 1 depicts the procedures of preparing the dynamics parameters described in Step 1.

Step 2: Apply the desired maneuvers such as changes of attitude angles and local-level velocity onto the nominal trajectory, and recompute the attitude angles, the local-level velocity vector, the geodetic locations, and other dynamic parameters that were obtained in Step 1. The vehicle maneuvers can be simplified as climb/descent with pitch change and turning with roll change:

$$\frac{d\theta}{dt} = \frac{A_z}{v_{xb}} \quad (13)$$

$$\frac{d\psi}{dt} = \frac{g\tan\phi_{\max}}{v_{xb}} \quad (14)$$

where A_z = vertical acceleration

v_{xb} = longitudinal velocity

$\phi_{\max}$ = maximum roll angle during turn, it can be achieved by a maximum roll rate before turning and can be reset by a reverse roll rate after turning.

The velocity in the local-level frame can be integrated via the following equation:

$$\begin{bmatrix} \dot{v}_n \\ \dot{v}_w \end{bmatrix} = \begin{bmatrix} \cos\theta\cos\psi & -\cos\theta\sin\psi & -\sin\theta\cos\psi \\ \cos\theta\sin\psi & \cos\theta\cos\psi & -\sin\theta\sin\psi \end{bmatrix} \begin{bmatrix} A_{xb} \\ v_{xb}\dot{\psi} \\ v_{xb}\dot{\theta} \end{bmatrix} \tag{15}$$

where v_n, v_w = north and west velocity

A_{xb} = longitudinal acceleration

$\dot{\psi}, \dot{\theta}$ = The total attitude rates, which combine equation (11) with equations (13) and (14).

ϕ, θ, ψ = the roll, pitch, and yaw angles are computed via integrating the attitude rates.

The new transformation matrix C_l^b can be computed from equation (8).

The geodetic latitude and longitude increments can be obtained from velocity components in north and west directions.

$$\begin{bmatrix} \Delta\Phi \\ \Delta\lambda \end{bmatrix} = \begin{bmatrix} \dfrac{v_n}{(R+h)} \\ \dfrac{-v_w}{(R+h)\cos\Phi} \end{bmatrix} \tag{16}$$

The transformation matrix C_e^l can be recomputed via equation (10) using the new geodetic location.

The transformation matrix C_i^b can be obtained from

$$C_i^b = C_l^b C_e^l C_i^e \tag{17}$$

For completeness, the body rates sensed by the gyro triad will be recomputed with the new craft rates and the new platform rates via the following equation:

$$\omega_{ib}^b = \omega_{ie}^b + \omega_{el}^b + \omega_{lb}^b = \Omega^b + \rho^b + \omega_{lb}^b \tag{18}$$

where the new platform rates $\omega_{lb}^b = (P, Q, R)^T$ can be updated by

$$\begin{bmatrix} P \\ Q \\ R \end{bmatrix} = \begin{bmatrix} -\dot{\psi}\sin\theta + \dot{\phi} \\ \dot{\psi}\cos\theta\sin\phi + \dot{\theta}\cos\phi \\ \dot{\psi}\cos\theta\cos\phi - \dot{\theta}\sin\phi \end{bmatrix} \tag{19}$$

and the craft rates can be computed by equation (5).

The new acceleration sensed by the accelerometer triad can be recomputed by

$$A = \left[{dv}/{dt} \right]_l + (\rho + 2\Omega) \times v - g \tag{20}$$

where all the input parameters were defined in equation (4).

Step 3: Transform the position in geodetic coordinates back to the inertial frame.

Other than the body rates, ω_{ib}^b, the acceleration, A_i, and the transformation matrix, C_i^b, already computed in Step 2, the position in the ECI frame can be obtained from

$$\begin{bmatrix} x_i \\ y_i \\ z_i \end{bmatrix} = \begin{bmatrix} \cos\Omega t & -\sin\Omega t & 0 \\ \sin\Omega t & \cos\Omega t & 0 \\ 0 & 0 & 1 \end{bmatrix} \begin{bmatrix} x_e \\ y_e \\ z_e \end{bmatrix} \tag{21}$$

Figure 2 depicts the procedures of generating the dynamics parameters described in Steps 2 and 3.

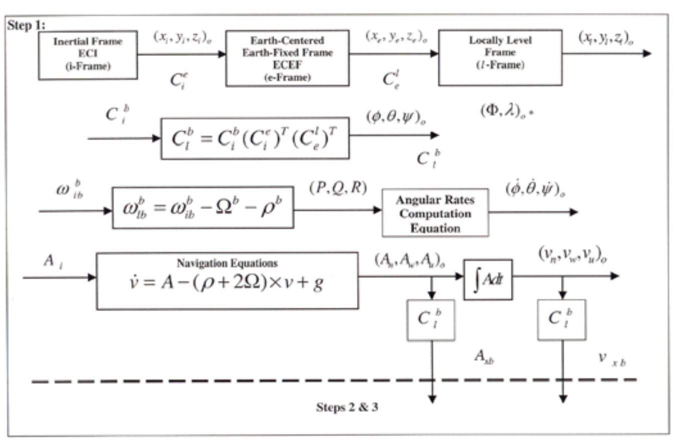

Figure 1. Block Diagram of Step 1 of Algorithm

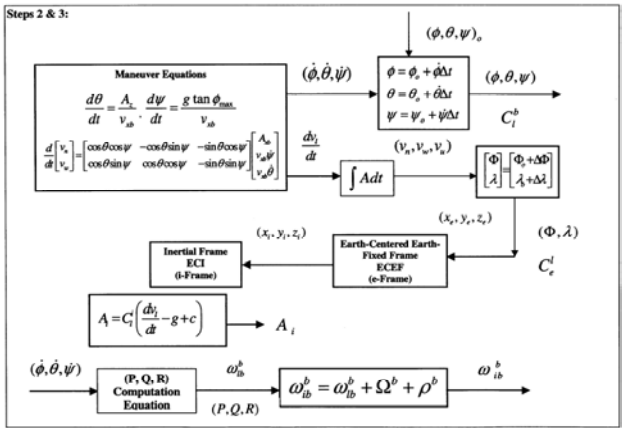

Figure 2. Block Diagram of Steps 2 and 3 of Algorithm

3. SIMULATION CONDITIONS

Based on the three-step algorithm, an off-nominal trajectory analysis tool has been developed on the Matlab platform to generate the trajectories that can be input to the dynamic link analysis tool. For demonstration purposes, a fictitious trajectory of a space vehicle that was launched from Disneyland in Anaheim and flew along the west coast is selected as the nominal trajectory. A fictitious location in the Los Angles area is selected as the command destruct site. The off-nominal trajectory is generated to model a vehicle that experiences a loss of control. It is deviated from the nominal trajectory, at 18 seconds from lift-off by spinning the vehicle at a constant rate of 4.5 deg/sec with respect to the yaw axis for 270 seconds.

To ensure that the command uplink can be closed with sufficient link margin under the conditions of a vehicle that experiences a loss of control, a thorough link analysis is required. The off-nominal trajectory is input to the dynamic link analysis tool to compute link margin versus time. The dynamic link analysis tool was developed as part of the overall performance evaluation of the complete SLR-CDS system.

The link margin (LM) can be computed from the link analysis tool based on the following formula [4]:

$$LM = \frac{EIRP\left(G_r\right)}{\left(\dfrac{S}{N}\right)_{\mathrm{Re}q} B_w k T_s L_s L_0} \tag{22}$$

where $EIRP = G_t P_t$ with transmitter loss included in L_o

$P_t =$ the transmitted power

$G_t =$ the transmit antenna gain

$G_r =$ the vehicle receive antenna gain, to be computed from receive antenna patterns along the trajectory

$B_w =$ the noise bandwidth of 180 KHz

$T_s =$ the receiver's system temperature

$k =$ Boltzmann's constant

$L_s =$ space loss, to be computed along the trajectory

$L_o =$ other losses of 5 dB

$\left(S/N\right)_{req} =$ required signal-to-noise ratio to achieved certain detection rate [5].

The vehicle antenna gain will be computed using several simulated vehicle antenna radiation patterns corresponding to different stages of the flight. A set of nominal link parameters is used in this simulation for demonstration purposes, and they are subject to change when modeling of the actual CDS system is required.

One very important parameter in the space vehicle link analysis is the plume attenuation caused by the burning fuel exhausted from the rocket propulsion system. The results obtained in [6] are employed in this analysis, which provide a good approximation of the true attenuation.

4. SIMULATION RESULTS

The ground traces of the nominal and off-nominal trajectories are shown in Figure 3, and their zoom-in plots are shown in Figure 4. The dynamic link analysis tool takes into consideration the dynamics of launch vehicle trajectories, free space loss, antenna gains, and plume attenuation. The dynamics of vehicles in turn include vehicle trajectory (position, velocity and acceleration) and vehicle orientation (attitude angles and attitude rates). Knowledge of the ground station and vehicle trajectory permits one to compute the slant range vector and the elevation angle from the ground station to the vehicle. For a given point in time, the free space loss can be estimated using the actual slant range. Figure 5 shows the slant range and the space loss versus time for the nominal trajectory and the off-nominal trajectory. The elevation angle to the vehicle should be greater than a threshold to ensure visibility from the ground station. During flight, the orientation of the vehicle is constantly changing with respect to the ground station. Dynamic angle parameters, describing launch vehicle characteristics relative to the ground station, are used to determine plume attenuation, the transmit antenna gain, and vehicle-receiving antenna gain along the line of sight.

Since the vehicle-receiving antennas are fixed on the vehicle, the peak of the antenna pattern is not always pointed to the ground station. The cone and clock angles describing antenna and vehicle orientation relative to the ground station are used to determine the instantaneous antenna gain. The antenna pattern cone angle is the angle between the slant range vector and the positive roll axis of the vehicle. The antenna pattern clock angle is the clockwise angle between the negative yaw axis and the projection of the slant range vector onto the roll plane when looking forward [7]. Figure 6 shows the cone angles, the clock angles, and the vehicle antenna gains for the nominal trajectory and the off-nominal trajectory. The antenna nulls from both trajectories can be as deep as -20dB, depending on vehicle orientation relative to the ground station.

If the aspect angle between the slant range vector and the negative roll axis (tail) is sufficiently large, then the plume attenuation is insignificant. However, for small aspect angles, the plume attenuation can be very significant. Figure 7 shows the aspect angles and the plume attenuation for the nominal trajectory and the off-nominal trajectory. The plume attenuation in the nominal trajectory is significant due to the small aspect angle, and a relatively large aspect angle can be observed in the off-nominal trajectory. Once the computation is performed, the results of the link margin versus time is available for analysis. Figure 8 shows the link margins for the nominal trajectory and the off-nominal trajectory. The negative link margin in the nominal trajectory is caused by the combined effect of the deep antenna null and the plume attenuation. However, the uplink of the off-nominal trajectory can be closed throughout the flight (except for a short duration) due to the fact that the significant plume attenuation only appears for a short period of time and did not aggravate the effect of deep antenna nulls.

5. Summary and Conclusions

This paper presents a three-step algorithm that is developed to model an off-nominal trajectory. Based on the algorithm, a software tool has been developed to generate the off-nominal trajectories. For demonstration purposes, the software was used to simulate a trajectory of a vehicle that has lost control, which is spinning with a constant yaw rate. The off-nominal trajectory was input to the dynamic link analysis tool to compute the link margin. The link margin of the off-nominal trajectory has been analyzed and compared against the link margin of the nominal trajectory. In the current simulation, the command uplink of the off-nominal trajectory can be closed with sufficient margin, while the link in the nominal trajectory is not always able to close. The negative link margin is caused by the combined effect of the deep antenna null and the plume attenuation.

The off-nominal trajectory analysis tool has been developed as part of the overall performance evaluation of the complete SLR-CDS system. This tool provides a powerful capability for system analysts to decide the destruct lines and perform engineering trade studies over a wide range of trajectories.

References

[1] D. Villalpando and R. Lucas, *UHF Command Destruct Link Analysis Report for the Eastern and Western Spacelift Range,* V.I, TOR-95(5496)-3 Revision 1, The Aerospace Corporation, June 1998.

[2] T. M. Nguyen, *Modeling of the SpaceLift Range System: A Command Destruct Subsystem*, to be published in IEEE Aerospace Conference, Big Sky, MT, March 2003.

[3] G. Siouris, *Aerospace Avionics Systems - A Modern Synthesis*, Academic Press, 1993.

[4] B. Sklar, *Digital Communication, Fundamentals and Applications*, Prentice Hall, Englewood Cliffs, NJ, 1988.

[5] R. Kumar, *Performance Analysis of a Command Destruct Subsystem of the Spacelift Range System*, to be published in IEEE Aerospace Conference, Big Sky, MT, March 2003.

[6] H. Poehler, *Rocket Exhaust Signal Attenuation and Degradation Final Report*, Vol. 1, ETR-TR-69-4, July 1969, Pan American World Airways, Aerospace Services Division, Patrick Air Force Base, Florida.

[7] *RF Link Analysis for the Titan IVB Core Vehicle for Western Range Flights*, Report Number: FCNX-BC/99-001, February 9, 1999, Lockheed Martin Astronautics, and Space Launch Systems

Biographies

Joseph C. Chen *received his M.S. and Ph.D. degrees in Mechanical, Aerospace, and Nuclear Engineering from the University of California, Los Angeles. Presently, he is an Engineering Specialist in the Communication Systems Subdivision of The Aerospace Corporation. Before joining Aerospace in 1996, he was with Litton Corporation from 1978 to 1987, Northrop Grumman Corporation from 1987 to 1996. His current interests include dynamic link analysis, digital signal processing, end-to-end communication systems analysis, GPS interference suppression using STAP/SFAP, and guidance, navigation, and control systems analysis.*

Charles C. Wang *received his M.S. and Ph.D. degrees in Electrical Engineering from the University of California, Los Angeles. Presently, he is the Manager of the Analysis & Networking Section in The Aerospace Corporation Communication Systems Subdivision. Before joining Aerospace in 1996, he was with LinCom Corporation from 1979 to 1981, the Jet Propulsion Laboratory from 1981 to 1990, TriLite Technology Corporation from 1991 to 1994, and the National Space Program Office in Taiwan from 1995 to 1996. His current interests include channel coding, bandwidth-efficient modulation, spread spectrum, network, and other areas in satellite communication systems*.

Dr. David Taggart *received his B.S., M.S., and Ph.D. degrees in Engineering from the University of California, Los Angeles with an emphasis on electrical engineering. Presently, he is a Senior Engineering Specialist in the Communication Systems Engineering Department in The Aerospace Corporation Communication Systems Subdivision. Before joining Aerospace in 1979, he was with TRW Systems from 1972 to 1979, and Hughes (Satellite Communications) from 1968 to 1972. His current interests include launch vehicle communication systems, digital signal processing and communications analysis and simulations, Homeland Security communications, and satellite communication systems.*

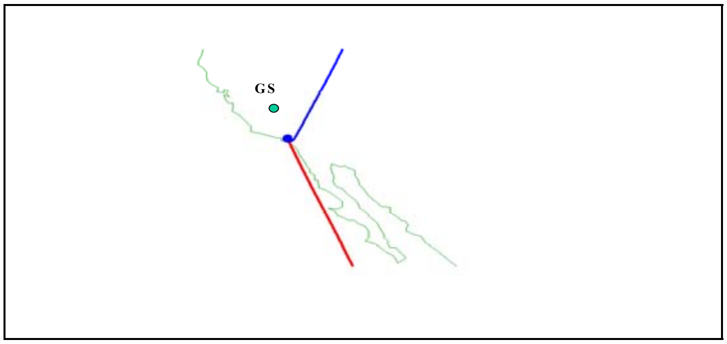

Figure 3. Ground traces of the nominal (red) trajectory and off-nominal (blue) trajectory (GS=ground station)

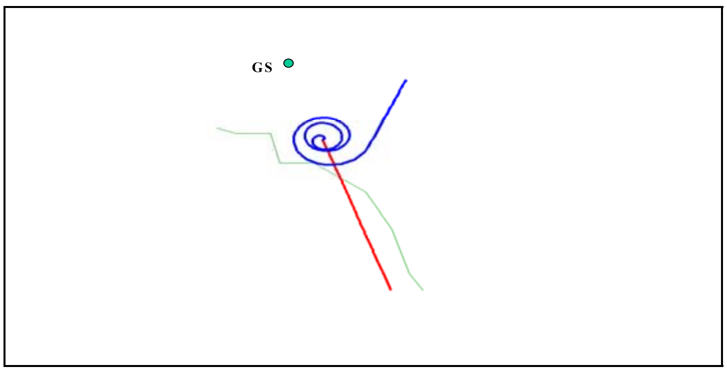

Figure 4. Zoom-in of nominal (red) trajectory and off-nominal (blue) trajectory (GS=ground station)

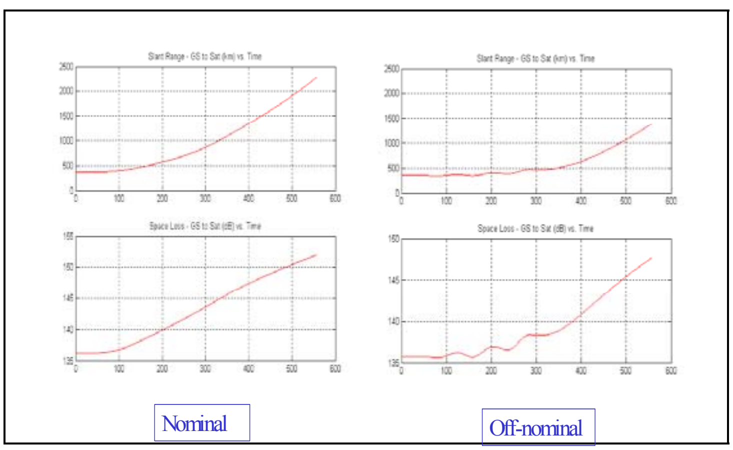

Figure 5. Slant range (Km, top) and space loss (dB, bottom) vs. time (sec) for nominal (left) and off-nominal (right) trajectories (Sat=satellite or launch vehicle)

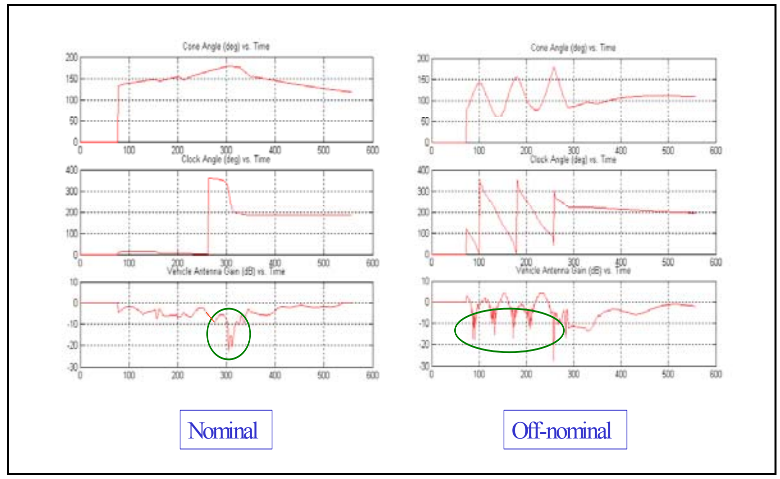

Figure 6. Cone angle (deg, top), clock angle (deg, middle), vehicle antenna gain (dB, bottom) vs. time (sec) for nominal (left) and off-nominal (right) trajectories

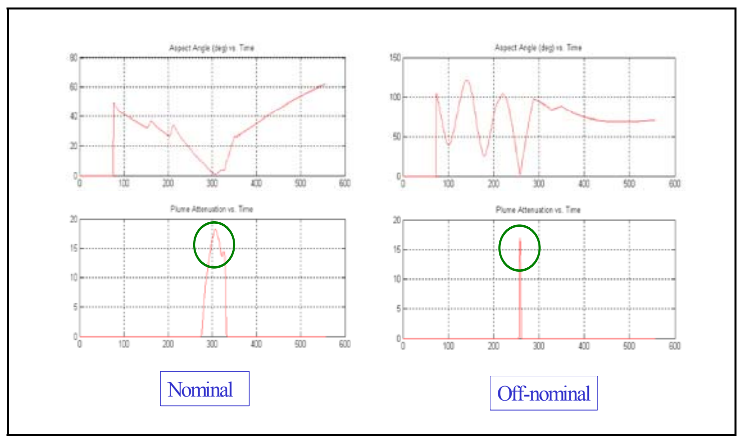

Figure 7. Aspect angle (deg, top) and plume attenuation (dB, bottom) vs. time (sec) for nominal (left) and off-nominal (right) trajectories

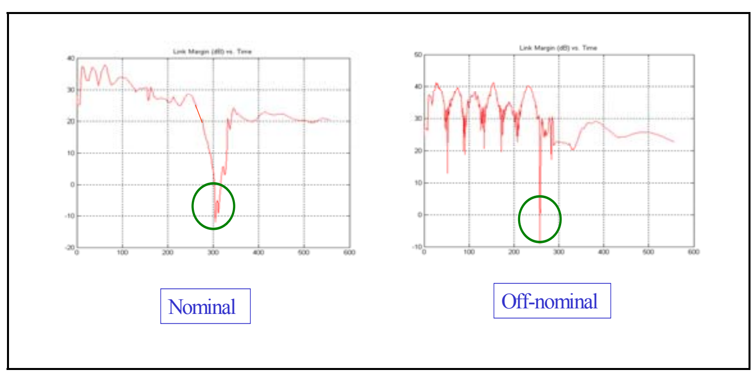

Figure 8. Link Margin (dB) vs. time (sec) for nominal (left) trajectory and off-nominal (right) trajectory